LETTERS
PUBLISHED ONLINE: 25 MARCH 2012 | DOI: 10.1038/NMAT3280
nature materials

A super-oscillatory lens optical microscope for subwavelength imaging

Edward T. F. Rogers[1], Jari Lindberg[2], Tapashree Roy[1], Salvatore Savo[1], John E. Chad[3], Mark R. Dennis[2] and Nikolay I. Zheludev[1]*

The past decade has seen an intensive effort to achieve optical imaging resolution beyond the diffraction limit. Apart from the Pendry–Veselago negative index superlens[1], implementation of which in optics faces challenges of losses and as yet unattainable fabrication finesse, other super-resolution approaches necessitate the lens either to be in the near proximity of the object or manufactured on it[2–6], or work only for a narrow class of samples, such as intensely luminescent[7,8] or sparse[9] objects. Here we report a new super-resolution microscope for optical imaging that beats the diffraction limit of conventional instruments and the recently demonstrated near-field optical superlens and hyperlens. This non-invasive subwavelength imaging paradigm uses a binary amplitude mask for direct focusing of laser light into a subwavelength spot in the post-evanescent field by precisely tailoring the interference of a large number of beams diffracted from a nanostructured mask. The new technology, which—in principle—has no physical limits on resolution, could be universally used for imaging at any wavelength and does not depend on the luminescence of the object, which can be tens of micrometres away from the mask. It has been implemented as a straightforward modification of a conventional microscope showing resolution better than $\lambda/6$.

The new imaging idea exploits the recently predicted[10,11] and observed[12] effect of optical super-oscillation. The key element of this new super-resolution technology is a super-oscillatory lens (SOL), a nanostructured mask that, on illumination with a coherent light source, creates a focus at a distance beyond the near-field of the mask. The ability to focus beyond the diffraction limit[13–15] is related to the fact that band-limited functions are able locally to oscillate arbitrarily quickly, faster than their highest Fourier components, a phenomenon now known as super-oscillation[10,16,17]. Whereas a conventional lens can only focus to a spot size of about a wavelength in diameter, a SOL can—in principle—create a focus of any prescribed size[18]. In all cases, however, as well as the subwavelength hotspot in a low-intensity super-oscillatory region, a larger high-intensity halo is simultaneously created. This limits the field of view of this focusing device in imaging. Furthermore, the subwavelength hotspots will only receive a minute fraction of the total power[16]. These features of the super-oscillatory hotspots have previously been seen as the main obstacles to imaging applications, aggravated by the technological problem of manufacturing a super-oscillatory mask with precise, continuous, coordinate-dependent retardation and transmission[19].

Two factors have allowed the imaging with super-oscillatory focusing that we report here. First, instead of a continuous mask, we have developed an easy-to-manufacture high-throughput binary SOL, a sequence of concentric rings of different width and diameter that ensures the accurate constructive interference of waves, leading to the subwavelength hotspot. Unlike previous work[20–23], super-oscillatory binary masks do not use evanescent waves to form subwavelength hotspots, and focus at distances tens of wavelengths away from the mask.

Second, for imaging we used a scanning mode with SOL illumination where the signal used to reconstruct the image is taken from the central part of the CCD detector; the region where the hotspot is projected in the absence of the object. This imaging tactic, also employed in confocal microscopy, allows the removal of unwanted scattering from the halo.

If a point-like source is imaged by a conventional lens, closing the aperture will gradually reduce the spot size and lens resolution. With a SOL, obscuring only a small part of its aperture could completely destroy the hotspot, which is formed by a very delicate balance of the interference of a large number of beams. On the other hand, this fragility of super-oscillation allows us to achieve resolution beyond that of the super-oscillatory spot size: even an obstacle smaller than the spot size will dramatically disturb this interference balance and, thus, the signal used for image reconstruction.

To design the binary mask the radial coordinate was divided into N concentric annuli, each of which had either unit or zero transmittance. The mask was optimized using the binary particle swarm optimization[24]. This is a nature-inspired evolutionary algorithm for stochastic optimization in which the swarm consists of a certain number of particles that move in the N-dimensional search space to find the global optimum. In contrast with algorithms assuming a fixed number of annuli[14,15], here the number can vary during the optimization process. We define the merit function for optimization as the size of the central spot. Furthermore, we constrain the solution space by requiring the usable field of view and the halo intensity to have experimentally feasible values. In applying the algorithm we used a swarm of 60 particles and 10,000 iterations with $N = 100$ and arrived at a SOL design (Fig. 1a) comprised of 25 transparent regions of varying size (see Supplementary Table S1 for full details of the SOL dimensions).

The ring pattern of the SOL (Fig. 1a) with outer diameter 40 μm was manufactured by focused ion-beam milling of a 100-nm-thick aluminium film supported on a round glass substrate and mounted as a microscope illuminating lens. When illuminated with a laser at $\lambda = 640$ nm, it generates a focal hotspot 185 nm in diameter, located at a distance of 10.3 μm from the film (Fig. 1b,c). The intensity of light in the SOL hotspot was ~25 times the intensity of the incident light. The sample was illuminated with the SOL installed in place of the conventional immersion

[1]Optoelectronics Research Centre and Centre for Photonic Metamaterials, University of Southampton, Southampton SO17 1BJ, UK, [2]H. H. Wills Physics Laboratory, University of Bristol, Bristol BS8 1TL, UK, [3]Institute for Life Sciences, University of Southampton, Southampton SO17 1BJ, UK.
*e-mail: n.i.zheludev@soton.ac.uk.

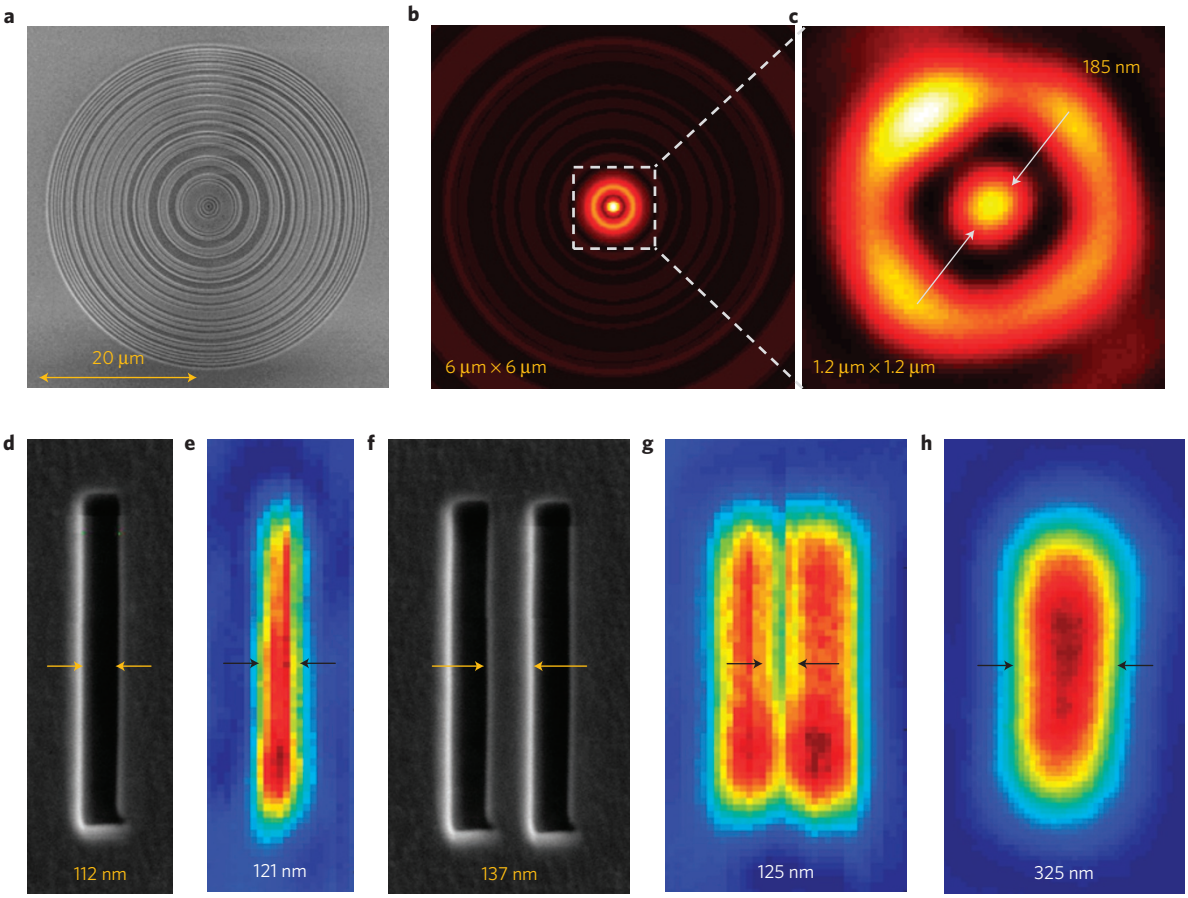

Figure 1 | Subwavelength imaging with a super-oscillatory lens. a, SEM image of the SOL. **b**, Calculated energy distribution of the super-oscillatory lens at 10.3 μm from the lens. **c**, The actual focal point, $\lambda = 640$ nm. **d**–**g**, SEM image of a 112 nm slit (**d**) and its SOL image (**e**); a double slit (**f**) and its SOL image (**g**). **h**, The image of the same double slit is not resolved using a conventional lens of NA = 1.4.

microscope lens. Imaging experiments were performed with a Nikon dual microscope. A diode laser with a single longitudinal mode operating at 640 nm was used as the source. The transmitted signal was recorded on a charge-coupled device (CCD) through a Nikon immersion microscope lens (model VC100xH). We used a fast frame rate 16-bit resolution 5 megapixel Andor Neo sCMOS camera. The object was scanned with 20 nm (Fig. 1) or 50 nm (Fig. 2) step across the spot using a X–Y nano-precision piezo stage. To construct the image, the detection zone was chosen to be a factor of three smaller than the hotspot image on the CCD. The image is reconstructed in a simple point-to-point consecutive scanning process without any deconvolution or post-processing, so no prior information about the sample is required.

As test objects to demonstrate optical resolution we used single and double nanoslits manufactured in a 100 nm titanium film (Fig. 1). A single slit 112 nm wide is seen by the SOL as a 121 nm slit (Gaussian fit). A 137 nm gap between two slits is well resolved and seen as a 125 nm gap (double Gaussian fit). These slits are not resolved by a conventional liquid immersion lens with NA = 1.4 (Fig. 1h). These measurements demonstrate a resolution of better than $\Delta \approx 140$ nm, or $\lambda/4.6$, which surpasses that of the near-field plasmonic superlens ($\lambda/3.6$; ref. 2) and 3D hyperlens ($\lambda/2.6$; ref. 3).

To demonstrate the ability of the super-oscillatory lens to image complex objects, we have fabricated a cluster of eight nanoholes in a 100 nm gold film (Fig. 2a) with widely varying hole separations. Details of the structure are blurry and not resolved in a conventional microscope image (Fig. 2b), but on the image taken with the super-oscillatory lens all the major features of the cluster are sharp and resolved: holes separated by 105 nm ($\lambda/6$) are seen as clearly distinct and separated. Moreover, two holes spaced by 41 nm ($\lambda/15$) are nearly resolved (Fig. 2c).

These images indicate that scattering from the halo sidebands into the detection area is not a significant problem owing to its small area and results in just visible halos around the imaged nanoholes (Fig. 2c). Here, small discrepancies between the scanning electron microscope (SEM) and SOL images are due to mechanical drifts in the microscope system during the scanning process, which takes about 600 s for the 2.75 μm × 2.75 μm sample area.

To further illustrate the experimentally demonstrated resolution, we compared recorded images against those obtained by computer modelling using the angular spectrum method[25] (Fig. 3). Modelling returned the focal spot of the SOL to be 185 nm in diameter, which agrees with the experimentally observed value (Fig. 1c). A comparison between simulated and experimentally recorded images is presented in Fig. 3. It demonstrates a very good agreement in resolution and shape, where the discrepancies are mainly due to the pixelation and CCD noise.

To investigate the effect of noise on image reconstruction, we simulated adding increasing levels of noise to the confocal detector, thus modelling a situation when a noisy laser is used or a less intense super-oscillatory hotspot is exploited. For the images presented in Figs 1 and 2 the dark field noise level was about 0.3% of the hotspot peak signal. The image presented in Fig. 4a is a simulated image of the hole cluster in Fig. 2a assuming zero noise. It maps perfectly on the SEM image (Fig. 2a) and the experimentally recorded SOL image (Fig. 2c). Images presented

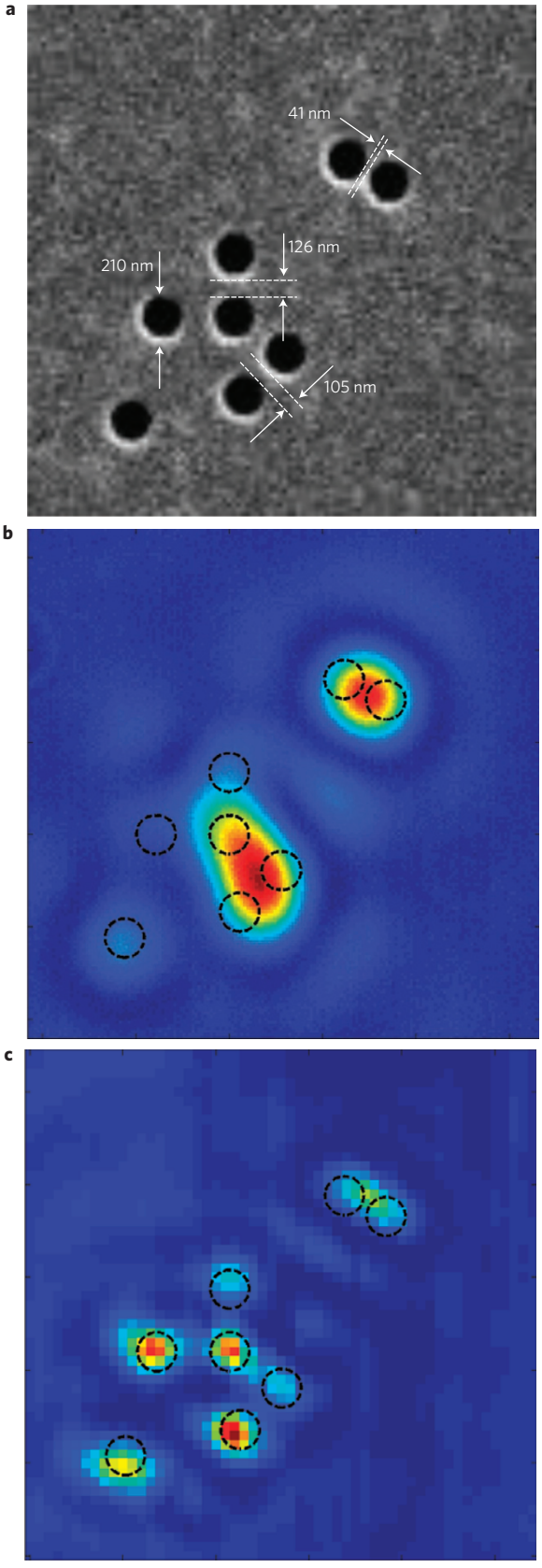

Figure 2 | Super-oscillatory imaging of complex objects. **a**, 2.75 μm × 2.755 μm SEM image of a cluster of nanoholes in a metal film. **b**, The image of the cluster is not resolved with a conventional lens of NA = 1.4. **c**, The SOL image resolves all the main features of the cluster. Dashed circles map the positions of the holes.

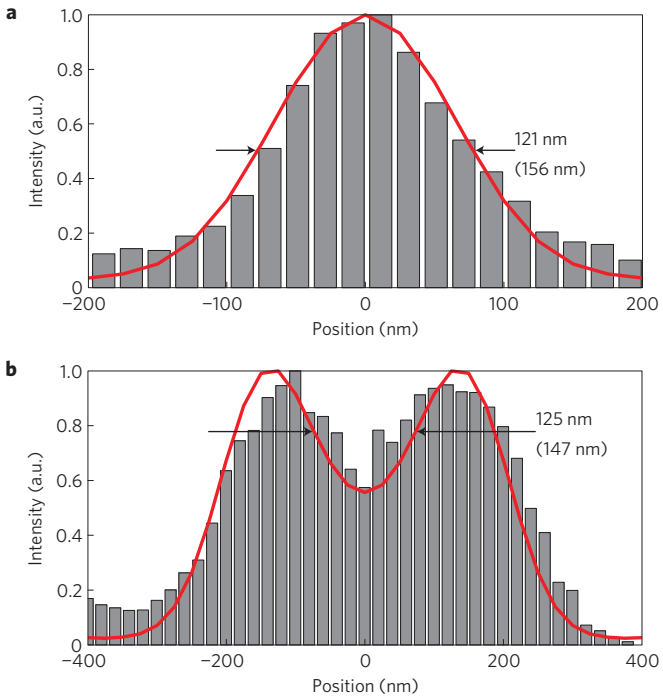

Figure 3 | Super-oscillatory imaging: experiment versus modelling. Experimentally recorded cross-sections of the SOL images (bars) and corresponding modelling results (solid lines). **a**, Results for the single-slit image presented in Fig. 1e. **b**, Results for the double-slit image presented in Fig. 1g. The half-widths of the single slit and the gap between the two slits are given in the figure, with the computed value in brackets. $\lambda = 640$ nm.

in Fig. 4b,c are simulated for normally distributed photo-detector noise with a standard deviation of 2 and 10% of the hotspot peak signal, respectively. They show the excellent resilience of the reconstruction process to the intensity fluctuations and detector noise. The main effect of noise seems to be the reduction of contrast in the image.

In conclusion, we argue that super-oscillation-based imaging has unbeatable advantages over other technologies. It is non-invasive, allowing the object to be at a substantial distance from the lens, and can operate at any wavelength from X-rays to microwaves. Furthermore, we are confident that the resolution of the SOL imaging can be improved even further by refining the design and increasing the size of the super-oscillatory mask and by increasing the dynamic range of the light detection so that smaller hotspots can be exploited.

Received 23 December 2011; accepted 17 February 2012; published online 25 March 2012

References

1. Pendry, J. B. Negative refraction makes a perfect lens. *Phys. Rev. Lett.* **85,** 3966–3969 (2000).
2. Zhang, X. & Liu, Z. Superlenses to overcome the diffraction limit. *Nature Mater.* **7,** 435–441 (2008).
3. Rho, J. *et al.* Spherical hyperlens for two-dimensional sub-diffractional imaging at visible frequencies. *Nature Commun.* **1,** 143 (2010).
4. Smolyaninov, I. I., Hung, Y-J. & Davis, C. C. Magnifying superlens in the visible frequency range. *Science* **315,** 1699–1701 (2007).
5. Lee, J. Y. *et al.* Near-field focusing and magnification through self-assembled nanoscale spherical lenses. *Nature* **460,** 498–501 (2009).
6. Wang, Z. *et al.* Optical virtual imaging at 50 nm lateral resolution with a white-light nanoscope. *Nature Commun.* **2,** 218 (2011).
7. Hell, S. W. Toward fluorescence nanoscopy. *Nature Biotech.* **21,** 1347–1355 (2003).
8. Huang, B., Wang, W., Bates, M. & Zhuang, X. Three-dimensional super-resolution imaging by stochastic optical reconstruction microscopy. *Science* **319,** 810–813 (2008).

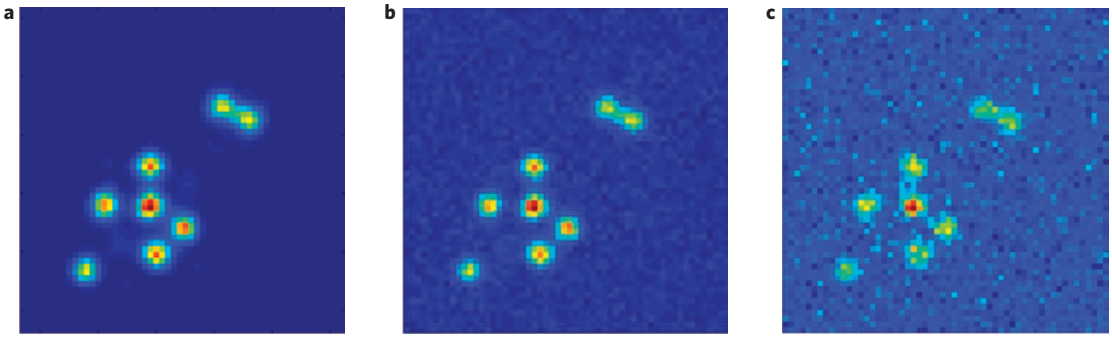

Figure 4 | The effect of noise on imaging. a, Simulated image of the hole cluster in Fig. 2a under zero noise conditions. Compared with the experimental image in Fig. 2c. **b**,**c**, Simulated images assuming detector/laser noise with a standard deviation of 2 and 10% of the peak hotspot signal, respectively, show the robustness of the imaging technique.

9. Gazit, S., Szameit, A., Eldar, Y. C. & Segev, M. Super-resolution and reconstruction of sparse sub-wavelength images. *Opt. Express* **17,** 23920–23946 (2009).
10. Berry, M. V. & Popescu, S. Evolution of quantum superoscillations and optical superresolution without evanescent waves. *J. Phys. A* **39,** 6965–6977 (2006).
11. Kempf, A. Black holes, bandwidths and Beethoven. *J. Math. Phys.* **41,** 2360–2374 (2000).
12. Huang, F. M., Zheludev, N., Chen, Y. & Javier Garcia de Abajo, F. Focusing of light by a nanohole array. *Appl. Phys. Lett.* **90,** 091119 (2007).
13. Toraldo di Francia, G. Super-gain antennas and optical resolving power. *Nuovo Cimento. Suppl.* **9,** 456–438 (1952).
14. Hegedus, Z. S. & Sarafis, V. Superresolving filters in confocally scanned imaging systems. *J. Opt. Soc. Am. A* **3,** 1892–1896 (1986).
15. Wang, H., Shi, L., Lukyanchuk, B., Sheppard, C. & Chong, C. T. Creation of a needle of longitudinally polarized light in vacuum using binary optics. *Nature Photon.* **2,** 501–505 (2008).
16. Ferreira, P. & Kempf, A. Superoscillations: Faster than the Nyquist rate. *IEEE Trans. Signal Proces.* **54,** 3732–3740 (2006).
17. Yakir Aharonov, D. A. & Vaidman, L. How the result of a measurement of a component of the spin of a spin-1/2 particle can turn out to be 100. *Phys. Rev. Lett.* **60,** 1351–1354 (1988).
18. Zheludev, N. I. Super-gain antennas and optical resolving power. *Nature Mater.* **7,** 420–422 (2008).
19. Huang, F. M. & Zheludev, N. I. Super-resolution without evanescent waves. *Nano Lett.* **9,** 1249–1254 (2009).
20. Mote, R. G., Yu, S. F., Ng, B. K., Zhou, W. & Lau, S. P. Near-field focusing properties of zone plates in visible regime—new insights. *Opt. Express* **16,** 9554–9564 (2008).
21. Li, J-H., Cheng, Y-W., Chue, Y-C., Lin, C-H. & Sheu, T. W. The influence of propagating and evanescent waves on the focusing properties of zone plate structures. *Opt. Express* **17,** 18462–18468 (2009).
22. Li, J-H., Lin, C-H., Tsai, Y-J., Cheng, Y-W. & Sheu, T. W-H. Modulation of optical focusing by using optimized zone plate structures. *Opt. Express* **18,** 22772–22780 (2010).
23. Grbic, A., Merlin, R., Thomas, E. & Imani, M. Near-field plates: Metamaterial surfaces/arrays for subwavelength focusing and probing. *Proc. IEEE* **99,** 1806–1815 (2011).
24. Jin, N. & Rahmat-Samii, Y. Advances in particle swarm optimization for antenna designs: Real-number, binary, single-objective and multiobjective implementations. *IEEE Trans. Antenn. Propag.* **55,** 556–567 (2007).
25. O'Shea, D. C., Suleski, T. J., Kathman, A. D. & Prather, D. W. *Diffractive Optics: Design, Fabrication, and Test* (SPIE, 2004).

Acknowledgements

This work was supported by the UK's Engineering and Physical Sciences Research Council under the Basic Technology (EP/F040644/1) and Nanostructured Photonic Metamaterials (EP/G060363/1) Programmes. The authors thank K. Dholakia, M. Mazilu, Y. Chen and A. D. Boardman for fruitful discussions and J. Y. Ou for assistance with nanofabrication.

Author contributions

The principle of super-oscillatory imaging was suggested by N.I.Z. with contributions from M.R.D. and J.E.C.; J.L. and M.R.D. developed mathematical algorithms for designing the binary super-oscillatory lens and computed the lens design. T.R. nanofabricated the binary mask and test objects. Optical characterization and modelling of the super-oscillatory lens performance was undertaken by E.T.F.R., S.S. and T.R. E.T.F.R. and N.I.Z. designed the opto-mechanical construction of the imaging apparatus with contributions from J.E.C. E.T.F.R. wrote the imaging instrument software, performed the imaging experiments and data post-processing. N.I.Z. supervised the project and wrote the manuscript with contributions from all co-authors. All authors contributed to the discussions of results and planning of experiments.

Additional information

The authors declare no competing financial interests. Supplementary information accompanies this paper on www.nature.com/naturematerials. Reprints and permissions information is available online at www.nature.com/reprints. Correspondence and requests for materials should be addressed to N.I.Z.